

CG dinucleotide codon removal improves expression of HIV-1 reporter viruses in humanized mice

by

Mariana Alexandra Benitez Moreno

BS Biology, La Roche University, 2019

Submitted to the Graduate Faculty of the
Graduate School of Public Health in partial fulfillment
of the requirements for the degree of
Master of Public Health

University of Pittsburgh

2021

UNIVERSITY OF PITTSBURGH
GRADUATE SCHOOL OF PUBLIC HEALTH

This thesis was presented

by

Mariana Alexandra Benitez Moreno

It was defended on

April 16, 2021

and approved by

Robbie B. Mailliard, PhD, Assistant Professor, Infectious Diseases and Microbiology, Graduate
School of Public Health, University of Pittsburgh

Jeremy J. Martinson, DPhil, Assistant Professor, Infectious Diseases and Microbiology,
Graduate School of Public Health, University of Pittsburgh

Thesis Advisor: Zandrea Ambrose, PhD, Associate Professor, Microbiology and Molecular
Genetics, School of Medicine, University of Pittsburgh

Copyright © by Mariana Alexandra Benitez Moreno

2021

CG dinucleotide codon removal improves expression of HIV-1 reporter viruses in humanized mice

Mariana Alexandra Benitez Moreno, MPH

University of Pittsburgh, 2021

Abstract

Two replication-competent CCR5-tropic HIV-1 reporter constructs were developed that encode either nanoluciferase (nLuc) or a near-infrared fluorescent protein (iRFP) for *in vivo* imaging of HIV-1 infection in humanized mice. However, the original versions of these reporters had reduced expression after 5 weeks post-infection. We hypothesized that CG dinucleotides present in the reporter genes could lead to reduced expression. Thus, we eliminated all CG dinucleotides with synonymous mutations in the reporter genes. Our objectives were to measure the intensities of HIV-1 p24 and reporter expression in the spleens of humanized mice that were infected with the original or codon-optimized (CO) reporter viruses. We hypothesized that CO reporter viruses would have improved reporter expression and would correlate better with HIV-1 p24 staining. Spleens were collected from humanized mice that had been infected for 7-15 weeks with one of the original reporter viruses or one of the CO reporter viruses. Thin sections of spleen were stained with antibodies against HIV-1 p24 and nLuc. Immunofluorescence of p24, nLuc, and iRFP was measured by confocal microscopy and analyzed for fluorescence intensity and co-localization. The intensity of p24 expression was similar in the spleens of mice infected with original or the CO HIV-1 reporter viruses. This was consistent with plasma viremia levels remaining high for animals infected with either virus. In contrast, the intensity of reporter expression was greater in the spleens of humanized mice infected with CO HIV-1

reporter viruses compared to mice infected with original HIV-1 reporter viruses. The difference was greater for iRFP virus, which originally had 138 CG dinucleotides in the reporter gene, than for nLuc virus, which had 38 CG dinucleotides in the reporter gene. These results correlated with whole animal reporter imaging. These findings suggest that CG dinucleotide codon removal improves the expression of the reporter genes in HIV-infected spleen cells in humanized mice. The fluorescence imaging analysis successfully quantified the HIV-1 p24 and reporter gene expression in HIV-1 infected mice spleens that can be applicable in other studies. Future *in vivo* imaging studies will be performed using CO reporter viruses.

Table of Contents

Preface.....	viii
1.0 Introduction.....	1
2.0 Methods.....	9
2.1 Developing the HIV-1 reporter viruses for imaging virus replication and dissemination <i>in vivo</i>	9
2.2 Humanized CD34+ mouse model	9
2.3 Tissue fixation and sectioning.....	10
2.4 Immunofluorescence staining.....	11
2.5 Imaging analysis	11
3.0 Results	13
3.1 Development of reporter HIV-1	13
3.2 Removal of CG dinucleotides in reporter genes improved reporter HIV-1 expression <i>in vivo</i>	15
3.3 Removal of CG dinucleotides in reporter genes improved reporter HIV-1 expression in spleen cells of humanized mice	19
4.0 Discussion.....	23
4.1 Public Health Implications	24
5.0 Bibliography	25

List of Figures

Figure 1. Development of replication-competent HIV-1 reporter viruses.....	14
Figure 2. Design of experiments to characterize replication-competent HIV-1 reporter viruses in humanized mice.	15
Figure 3. Low correlation of plasma viremia with <i>in vivo</i> imaging of original HIV-1 reporter viruses.....	16
Figure 4. Codon optimization improves <i>in vivo</i> replication of HIV-1 reporter viruses.	18
Figure 5. Reporter gene expression can be detected in HIV-1 infected cells in the spleens of humanized mice.....	20
Figure 6. Expression of reporter proteins is improved in spleens of humanized mice infected with codon-optimized HIV-1 reporter viruses.	22

Preface

This thesis is the final work of my Master study at the University of Pittsburgh Graduate School of Public Health. It serves as a documentation of my research from January 2020 until February 2021. It specifically looks at how codon optimized reporters improve the expression of HIV-1 reporter viruses and its implications for public health. This project used the UPMC Hillman Animal Facility and the Center for Biological Imaging.

I wish to thank Dr. Chandra Nath Roy for production of NSG mice, whole animal imaging, and training imaging, Callen Wallace for help with imaging at the CBI, and Dr. Zandrea Ambrose for providing guidance through my laboratory experience and the preparation of my thesis. In addition, I thank Chris Kline for performing plasma viremia on the mice. Lastly, I would like to thank Dr. Jeremy Martinson, Dr. Robbie Mailliard, and Dr. Zandrea Ambrose for providing feedback and support through this process.

1.0 Introduction

The human immunodeficiency virus (HIV), which causes acquired immunodeficiency syndrome (AIDS), is one of the most serious health and development challenges in the world. Approximately 38 million people are currently living with HIV, and tens of millions of people have died of AIDS-related causes since the beginning of the epidemic (1). In 2019, 690,000 people died of AIDS-related causes and 1.7 million people were newly infected with HIV globally (2). In 2018, 37,968 people were diagnosed with HIV in the United States (U.S.) and U.S.-dependent areas (3). Of the new diagnoses in the US, 69% were among gay and bisexual men, 24% were among heterosexuals, and 7% were among people who injected drugs (3).

There was a 7% increase of HIV diagnoses from 2014-2018 among Black/African Americans in the U.S., showing that this subpopulation is disproportionately affected by HIV (4). Black/African American male-to-male sexual contact accounted for 37% of new diagnoses and Hispanic/Latino male-to-male sexual contact account for 30%, while White male-to-male sexual contact accounted for 27% of the new diagnosis (5). There is no effective cure for HIV, but with proper medical care, HIV replication can be suppressed.

According to the Centers for Disease Control and Prevention (CDC), of the estimated 1.1 million people living with HIV in the U.S. in 2018, 36% were aged 55 and older (4). When the HIV/AIDS epidemic started, infected individuals expected to live approximately one or two years. The reason there is a larger older population living with HIV is due to antiretroviral therapy (ART) that inhibits virus replication. Due to the improvements in the effectiveness of ART, people who are diagnosed early and use ART consistently can have long healthy lives. Consequently, nearly half of the people living with diagnosed HIV in the United States are aged 50 or older (4).

Having a longer life expectancy with HIV means that infected individuals are at risk for comorbidities. Despite effective antiretroviral therapy, many studies have suggested that HIV-1 may increase the risk of chronic comorbid diseases such as hyperlipidemia, atherosclerosis, and osteoporosis (6) (7). According to one study, researchers found that HIV-infected people 50 years and older who had received an AIDS diagnosis had a mean of 3.4 comorbidities (4). These comorbidities include cardiovascular disease, cancers, lung disease, and liver disease (including hepatitis C and hepatitis B). Preexisting cardiovascular, hepatic, and metabolic conditions are often complicated by HIV infection. In addition to susceptibility to comorbidities, older adults living with HIV are at risk of developing cancer (8). According to one study, people living with HIV experience a significantly higher incidence of cancer, including melanoma, leukemia, renal, anal, liver, lung, mouth, and throat cancers (9). The loss of the CD4⁺ T cells by HIV is the main reason for opportunistic infections and cancers associated with HIV infection.

HIV is transmitted primarily through blood and genital fluids. It can also be transmitted from infected mothers to newborn infants. People can become infected with HIV by direct contact with certain body fluids from a HIV-infected person. For transmission to occur, HIV in the fluids must come in direct contact with mucous membranes or damaged tissues, or be directly injected into the bloodstream of an HIV-negative person. Mucous membranes are found inside the mouth, rectum, vagina, and penis. Most HIV transmission occurs through anal or vaginal sex or sharing syringes (10).

HIV is a retrovirus; its genome consists of two identical single-stranded RNA molecules that are enclosed within the capsid of the virus particle. HIV replicates in and kills CD4⁺ T cells, which are an important part of the immune system. To enter a cell, HIV must bind and fuse with the host cell. The virus binds to the human CD4 receptor and a coreceptor (usually CCR5 or

CXCR4) on the host cell. After entry, the viral RNA is converted into DNA by reverse transcription. HIV DNA integrates into the host cell chromatin, which is an essential step in the retroviral replication cycle. At the chromosomal level, HIV integration is strongly favored in active transcription units, which promotes efficient viral gene expression (11). New HIV particles leave the host cell by budding and move on to infect other cells (12). Once HIV destroys enough of CD4+ cells, the immune system is not effective at combating basic infections and illnesses. Such opportunistic infections are more frequent and severe in people with weakened immune systems. When a person becomes infected with HIV, the virus attacks and weakens the immune system. During this time, the person is at risk of getting life-threatening infections and cancers. When that happens, the illness is called acquired immunodeficiency syndrome (AIDS). The HIV-infected person is said to have AIDS when they become sick with other specific opportunistic infections or when the number of CD4+ T cells has dropped below 200 cells/mm³ (13).

According to multiple studies, hyperimmune responses with production of pro-inflammatory cytokines, such as TNF- α , can lead to greater HIV production and damage of CD4+ and CD8+ T cells through apoptosis (14) and immune senescence (15). Immune senescence is the aging of the immune system and changes in lymphocytes development and function. Studies have shown the absence of the chronic activation in long-term nonprogressors, reflecting low viremia, and in natural nonpathogenic simian immunodeficiency virus (SIV) infection of monkeys, which have high viremia and no disease (16). These findings suggest that chronic activation leads to comorbidities. Thus, due to all the effects that HIV has on the body and immune system, it is important to curb the HIV epidemic.

The U.S. Department of Health and Human Services (DHHS) has launched *Ending the HIV Epidemic: A Plan for America*. DHHS is proposing this opportunity to eliminate new HIV

infections in the U.S. The initiative aims to reach 75% reduction in new HIV infections in 5 years and at least 90% reduction by 2030 (17). The multi-year program will include 48 counties, Washington, D.C., San Juan, Puerto Rico, as well as 7 states that have a substantial rural HIV burden with additional expertise, technology, and resources that they need to end the HIV epidemic. Collaborating agencies include the Centers for Disease Control and Prevention (CDC), Health Resources and Services Administration (HRSA), Indian Health Service (IHS), National Institutes of Health (NIH), Office of the HHS Assistant Secretary for Health, and Substance Abuse and Mental Health Services Administration (SAMHSA). Over a 10 year period, the initiative will scale up four science-based strategies that can end the epidemic: diagnose, treat, prevent, and respond. Diagnosis will focus on identifying all people with HIV as early as possible after infection. The treatment strategy will focus on providing treatments rapidly and effectively to achieve sustained viral suppression. Prevention will focus on making sure that people at risk for HIV use potent prevention interventions, including pre-exposure prophylaxis (PrEP) to prevent HIV transmission. Lastly, the respond strategy will focus on rapidly detecting and responding to growing HIV clusters of infection and preventing their spread to others (18).

A strategy to prevent and decrease the risk of transmission is the use of PrEP. This consists of HIV uninfected individuals taking a daily dose of antiretroviral drugs to lower their chances of acquiring HIV. PrEP has been proven to be effective among men who have sex with men, and CDC has issued interim guidance on its use in this population (19). Studies have also shown that PrEP is effective among heterosexual men and women (20). PrEP reduces the risk of acquiring HIV from sexual contact by about 99% when taken as prescribed (21). Among people who inject drugs, PrEP reduces the risk of HIV transmission by at least 74% when taken as prescribed (21).

While PrEP can play an important role in prevention of HIV, more understanding on how to better implement it in high risk populations is needed.

It is important for people to know their HIV status so they can take antiretroviral therapy (ART) to treat HIV if they are infected. The main goal of the treatment is to reduce the virus replication to an undetectable level. Taking ART every day can suppress viremia to undetectable levels. People who maintain viral suppression can live a long and healthy life (22). Because ART reduces HIV replication in the body, the immune system can be preserved and replenish CD4+ cells (23). In addition, suppressed individuals have effectively no risk of transmitting HIV to uninfected partners. A clinical trial showed that treating people living with HIV early after infection reduces the risk of transmitting the virus to others by 96 % (24).

Although ART can inhibit HIV replication and can prevent disease progression, it is not capable of curing HIV infection. The reason for this is that replication-competent HIV DNA can persist in cells during many years of ART. If ART is stopped, then HIV replication can continue again (25). Latently infected CD4+ T cells are the most studied HIV reservoirs, as they are numerous and can harbor integrated HIV DNA that can be induced with an appropriate stimulation of the cell (26) (27) (28). Studying these cells can be challenging due to relatively low frequencies in an ART-treated individual (approximately 1 infected cell per million CD4+ T cells) and their abundance in tissues that are hard to reach (29). To study CD4+ T cell latency, animal models of HIV/AIDS can be used.

An animal model for human disease should mimic the infection of humans as closely as possible (30). Animal models are essential for studying HIV-1 therapeutics regimens. The infection and treatment of patients cannot be controlled in clinical studies. Furthermore, certain procedures and sampling cannot be performed in humans because they might be difficult and

unethical. Animal models offer various advantages when it comes to study HIV/AIDS. The current types of models are mouse and non-human primate models. Mouse models offer high reproductive rates and low maintenance costs (31). These species are distantly related to humans, which means that obtaining results for a human disease is not always accurate. Non-human primates are used because they are more similar to humans. However, HIV cannot replicate in macaques, requiring the use of simian immunodeficiency virus (SIV). SIV is another lentivirus that is closely related to HIV. It is endemic in several non-human primate species in Africa, where it does not cause immune deficiency despite high levels of replication (32). Zoonotic transmission of SIV into humans has been described several times and has given rise to HIV type 1 and HIV type 2 (32). SIV infection in Asian macaques closely resembles HIV-1 infection in humans and leads to the development of opportunistic infections. However, SIV has significant differences from HIV (31).

Another useful way to study HIV is by using humanized mice. Humanized mice carry functioning human genes, cells, tissues, and/or organs. Humanized mice are commonly used as small animal models in biological and medical research for human therapeutics. We use this mouse because HIV requires human CD4+ cells in order to replicate and does not productively infect mouse cells (33). Therefore, introduction of human cells into mice is required for HIV infection and pathology. To allow replication of HIV in the mouse, scientists used severe combined immunodeficient (SCID) mice. They lack lymphocytes, but can be engrafted with human peripheral blood mononuclear cells (PBMCs) or human fetal thymus and liver (34). However, T cells were not detected to a great extent in the tissues. Another issue was that other human immune cells did not develop, and only transient HIV-1 replication could be detected *in vivo* (30). Multiple limitations pushed new advances in the humanized murine models that allowed the models to

reconstitute a human immune system and to lead to a sustainable HIV-1 replication (30). For example, NSG mice are extremely immunodeficient. They carry two mutations on the NOD/ShiLtJ genetic background: severe combined immune deficiency (*scid*) and a complete null allele of the IL2 receptor common gamma chain (*IL2rg^{null}*). The *scid* mutation is in the DNA repair complex protein *Prkdc* and renders the mice B and T cell deficient. The *IL2rg^{null}* mutation prevents cytokine signaling through multiple receptors, leading to a deficiency in functional NK cells. The severe immunodeficiency allows the mice to be humanized with tissues or cells (35). Human CD34+ hematopoietic stem cells introduced into NSG mice lead to the development of human lymphocytes and myeloid cells in the blood and in lymphoid tissues. Also, HIV-1 infection could be sustained at high levels for more than 40 days (36). This allows us to study HIV pathogenesis and treatment over a long period of time in animals.

Noninvasive imaging of viral pathogens in small animal models is a powerful tool used to monitor infection in real time. Imaging allows visualization of temporal and spatial progression of infection in real time. This is possible due to the high sensitivity and dynamic range of the bioluminescent and fluorescent reporter genes. Preserving the native viral genome structure as well as using small reporter genes ensures the proper replication of HIV reporter virus (37). A previous study demonstrated that noninvasive bioluminescent imaging of HIV encoding nLuc was possible (37). nLuc is an ideal candidate for imaging due to its relatively small sequence and its 150-fold brighter luminescence than fluorescent proteins (38). While it has a large dynamic range and a low background, it requires a substrate for imaging that is rapidly metabolized. We also sought to develop a fluorescent reporter virus, as it would not require a substrate and infected cells could be easily detected. The wavelengths of near-infrared fluorescent proteins range from 650 to 900 nm and their high brightness makes iRFP a remarkable tool to image in deep tissues (39).

Thus, we developed two replication-competent CCR5-tropic HIV-1 reporter constructs that encode either nLuc or iRFP for *in vivo* imaging in humanized mice. However, the original versions of these reporters had reduced reporter expression after 5 weeks post-infection despite high levels of plasma viremia. A previous study showed that high frequencies of CG dinucleotides in HIV-1 were associated with reduced virus replication due to recognition by the human zinc finger antiviral protein (ZAP) (40). In mammalian cells, ZAP depletes cytoplasmic RNA that is recognized as foreign due to its elevated CG dinucleotide content compared with endogenous mRNAs (41). We hypothesized that CG dinucleotides present in the reporter genes led to loss of reporter gene expression.

To test this hypothesis, CG dinucleotides were eliminated with synonymous mutations in the reporter genes to improve their expression *in vivo*. This led to improved *in vivo* imaging of nLuc and iRFP in mice infected with these codon-optimized (CO) reporter viruses. My objectives were to measure 1) the frequencies of cells that had detectable HIV-1 capsid (p24) staining cells as well as detectable iRFP or nLuc and 2) the intensities of p24, iRFP, and nLuc expression in the spleens of humanized mice that were infected with the original or the CO reporter viruses. Our expectation was that the CO reporter viruses would have improved iRFP/nLuc expression and would correlate better with HIV-1 p24 staining than the original viruses.

2.0 Methods

2.1 Developing the HIV-1 reporter viruses for imaging virus replication and dissemination in vivo

A proviral plasmid encoding HIV-1_{NL4-BAL} (42) was modified to encode nLuc or iRFP upstream of an internal ribosome entry site (IRES; 6ATRI) between *env* and *nef* using gene synthesis (GenScript) in the same manner previously described (43). Subsequently, the nLuc and iRFP genes were re-synthesized to remove all CG dinucleotides with synonymous mutations (CO viruses). Viruses were produced by transfection of HEK293T cells with proviral plasmids using Lipofectamine 2000 (ThermoFisher). Cell culture supernatant containing HIV-1 was filtered through a 0.45 µm filter, concentrated with Lenti-X (Takara), and frozen in aliquots at -80° C. Viruses were titered in duplicate on GHOST cells (44) by limiting dilution and flow cytometry on a BD Accuri flow cytometer (BD Biosciences).

2.2 Humanized CD34+ mouse model

All animal-related work was conducted according to the Public Health Services guidelines. Mice were housed at the University of Pittsburgh Division of Laboratory Animal Resources at the UPMC Hillman Cancer Center in accordance with the American Association of Accreditation of Laboratory Animal Care standards. All procedures were approved by the University of Pittsburgh Institutional Animal Care and Use Committee under protocol 17020145.

NSG mice reconstituted with human CD34+ cells were purchased from Jackson Laboratory. These mice were challenged intraperitoneally (IP) with 10^4 infectious units, as determined by the GHOST cell assay, of either nLuc HIV-1 or iRFP HIV-1. Plasma HIV-1 RNA was isolated regularly as previously described and quantified by SCA (45). At necropsy (3-12 weeks post-challenge), portions of spleen tissues were collected at necropsy from all viremic mice infected with an original reporter virus (n = 5-6/group) or a CO reporter virus (n = 4/group).

Plasma viremia and whole body imaging were performed by others in the Ambrose laboratory.

2.3 Tissue fixation and sectioning

Each tissue was placed in 2% paraformaldehyde and completely submerged in the solution for 1-2 hours. After the two hours, the tissue was submerged in 30% sucrose for 24 hours with the sucrose changed 2-3 times. A plastic beaker containing 2-methylbutane (Fisher) was placed in an ice bucket inside a styrofoam box containing a few inches of liquid nitrogen. Tissue samples were placed on a small piece of filter paper with forceps and completely immersed in the cooled 2-methylbutane for 30 seconds. The samples were removed from the beaker and immersed in the liquid nitrogen for an additional 10 seconds. Samples were placed into a cooled storage container and stored at -80°C until sectioning. Thin sections (10 μm) of spleen were cut with a microtome and kept at -20C until they were ready for use.

2.4 Immunofluorescence staining

Slides were rehydrated with 2 washes of phosphate buffered saline (PBS). Then, they were permeabilized with PBS containing 0.1% Triton X-100. Tissues were blocked with buffer containing 2% bovine serum albumin (BSA) and 20% donkey or goat serum for 45 minutes. Slides were washed 5 times with PBS containing 0.5% BSA (PBB). Staining was performed with antibodies against HIV-1 p24 (1:1500; Santa Cruz Biotechnology, clone 24-4) and nLuc (1:1000; R & D Systems, clone 965808) for 1 hour, followed by washing with PBB. Incubation with secondary antibody was performed for 1 hour with donkey anti-mouse IgG-Cy3 (1:2000; Jackson Immunological) or goat anti-mouse IgG-Cy5 (1:1500; Abcam). Slides were washed 5 times with PBB and 5 more times with PBS. Hoechst stain was added for 30 seconds to stain the nuclei and the sections were washed 5 times with PBS. To adhere the cover class over the sample, a drop of gelvatol was used. Slides were stored overnight in the dark to dry.

2.5 Imaging analysis

Immunofluorescence of p24, nLuc, and iRFP was measured by confocal microscopy. A Nikon A1 spectral inverted confocal microscope with a 40X 1.49 NS oil immersion objective (Nikon) was used to acquire images of the fixed tissue samples. LU-NV laser launch (Nikon) was used to emit lasers at 405 nm (Hoechst), 561 nm (Cy3), and 640 nm (Cy5/iRFP). For each tissue section, multiple images were acquired from different randomly chosen fields of view. NIS-Elements software (Nikon) was used to analyze fluorescence intensity and frequency of fluorescent cells. For analyzing *in vivo* HIV-1 reporter expression, the entire tissue area was

segmented based on Hoechst signal to define each segment as a cell with a nucleus. Then, for each respective channel (Cy3.5 for HIV-1 p24 and Cy5 for iRFP or nLuc), positive cells were determined. Cells having positive immunofluorescence were selected as binary zones, which were converted to regions of interest to measure mean fluorescence intensity of each positive cell with iRFP/nLuc and p24 signal. The total number of positive cells analyzed for nLuc and iRFP were 4131 and 3114, respectively. The total numbers of p24+ cells were 5011 (nLuc virus) and 4462 (iRFP virus). The average cell frequencies and intensities were determined by Prism (GraphPad) and the mean of the averages was plotted per group. Groups were compared using unpaired t tests for each measurement using Prism.

3.0 Results

The work described below is comprised of unpublished results recently submitted for publication:

Roy CN, Benitez Moreno MA, Kline C, Ambrose Z. CG dinucleotide removal in bioluminescent and fluorescent reporters improves HIV-1 replication and reporter gene expression for dual imaging in humanized mice, under review.

All tissue staining and analysis was performed by me. *In vivo* mouse work and microscopy was performed by Chandra Nath Roy. Molecular biology and plasma viremia measurements were performed by Christopher Kline.

3.1 Development of reporter HIV-1

To visualize HIV-infected cells *in vivo*, the CCR5-tropic replication-competent HIV-1_{NL4-BAL} molecular clone was engineered to express either nLuc or iRFP (nLuc HIV-1 or iRFP HIV-1, respectively; Figure 1), similar to a previously described construct [49]. The reporter genes were introduced upstream of the encephalomyocarditis virus internal ribosome entry site (IRES), 6ATRi, to allow expression of *nef*. While all viruses replicated with similar kinetics, reporter virus production, particularly for iRFP HIV-1, was reduced compared to WT HIV-1 (data not shown).

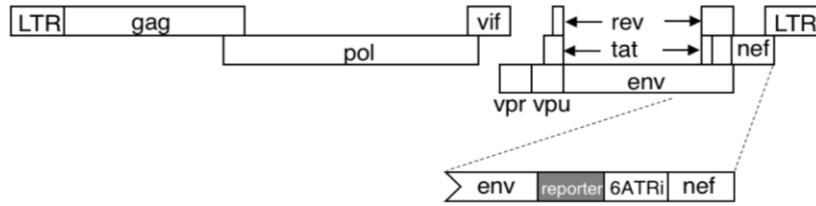


Figure 1. Development of replication-competent HIV-1 reporter viruses. A schematic of the HIV-1 genome shows the reporter gene (nLuc or iRFP) and the 6ATRi sequence between env and nef.

High frequencies of CG dinucleotides in HIV-1 have been shown to be associated with reduced virus replication due to recognition by human ZAP (40). We hypothesized that CG dinucleotides present in the nLuc and iRFP genes could lead to reduced virus replication and reporter gene expression. While the HIV-1 *gag* and *pol* genes (4509 bp) had a total of 26 CG dinucleotides, nLuc (516 bp) and iRFP (936 bp) had 38 and 138 CGs, respectively. Synonymous base substitutions were introduced into the reporter genes of nLuc HIV-1 and iRFP HIV-1 to remove all CGs. Although the 6ATRi IRES (461 bp) had 21 CG dinucleotides, these were not removed to avoid potentially affecting Nef expression. Replication of codon-optimized (CO) reporter viruses had similar replication compared to WT HIV-1 and improved replication compared to the original reporter viruses (data not shown), showing that fewer CG dinucleotides in the reporter viruses resulted in improved replication *in vitro*.

3.2 Removal of CG dinucleotides in reporter genes improved reporter HIV-1 expression *in vivo*

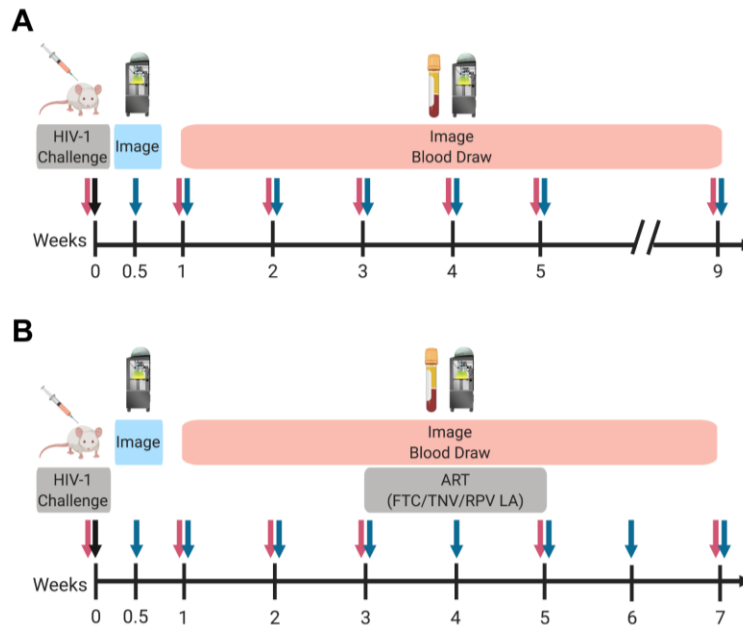


Figure 2. Design of experiments to characterize replication-competent HIV-1 reporter viruses in humanized mice. (A) Original or (B) codon-optimized nLuc HIV-1 or iRFP HIV-1 was injected IP into humanized mice. Virus replication was measured by qRT-PCR of viral RN.

To determine reporter virus replication *in vivo*, mice engrafted with human CD34+ hematopoietic stem cells were injected with either 104 infectious units of nLuc HIV-1 (n = 5) or iRFP HIV-1 (n = 6). HIV-1 RNA was quantified weekly in the plasma of the mice for 5 weeks post-challenge by quantitative RT-PCR (Figure 2A). A subset of mice was followed until 9-12 weeks post-challenge. nLuc HIV-1 infected 4/5 mice and iRFP HIV-1 infected all 6 mice, as measured by viral RNA present in the plasma (Figure 3A). Plasma viremia plateaued at week 4 post-infection in the majority of the mice and was maintained stably through at least 9 weeks post-infection, which was similar to wild-type HIV-1NL4-BAL infection of BLT mice (46).

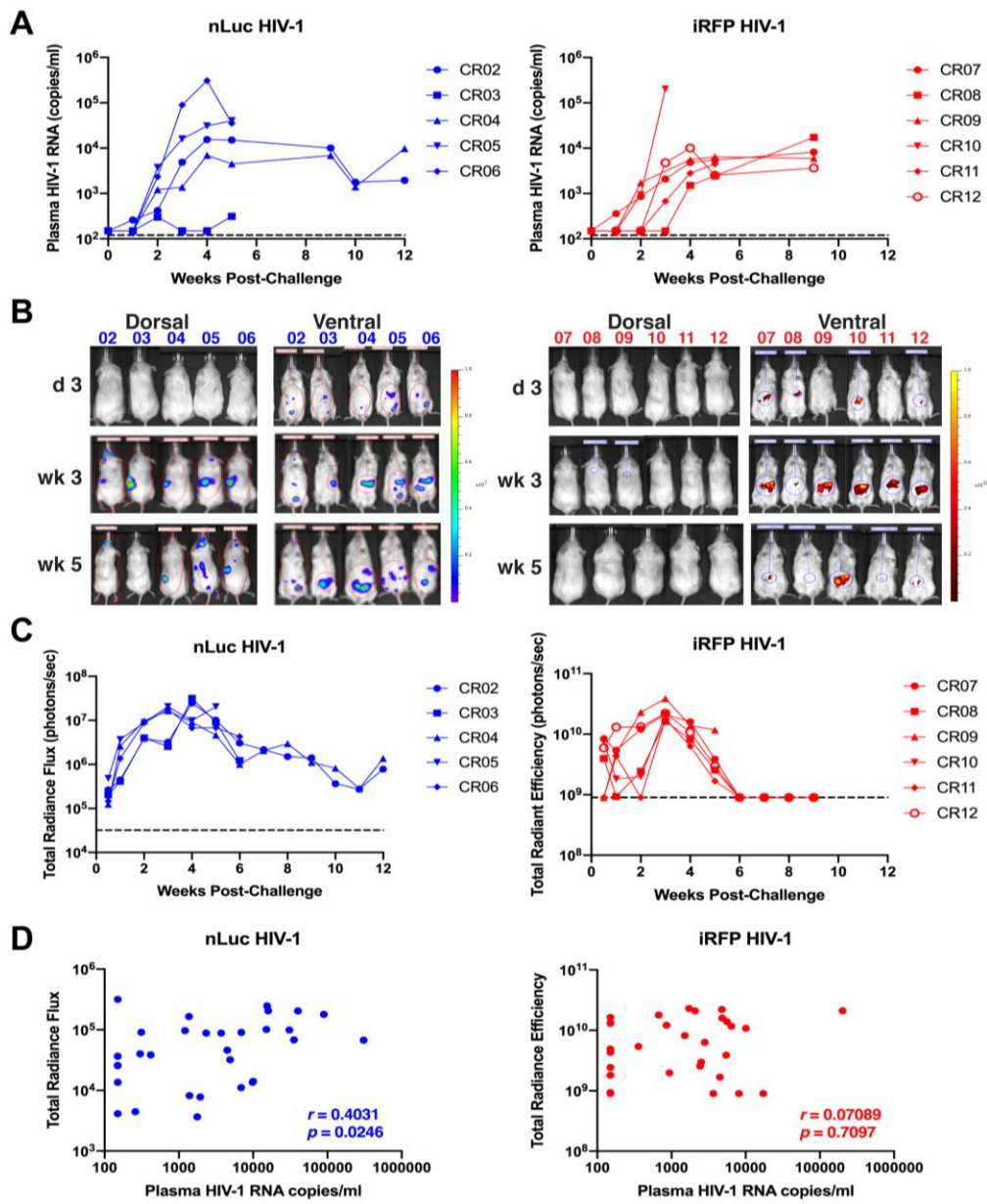


Figure 3. Low correlation of plasma viremia with *in vivo* imaging of original HIV-1 reporter viruses. Humanized mice were challenged with nLuc HIV-1 (n = 5) or iRFP HIV-1 (n = 6). (A) Plasma viremia was measured by qRT-PCR. The limit of detection is denoted by the dashed lines. (B) Images of *in vivo* nLuc or iRFP expression measured by whole body imaging. (C) Expression of *in vivo* nLuc and iRFP expression was quantified at each time point. The limit of detection above background signal for total radiance flux is denoted by dashed lines. (D) Correlations of reporter gene expression with plasma viremia for all time points are shown. Spearman's rank correlation coefficient (r) and p values are shown.

Whole animal imaging also was performed on the mice prior to infection, 3 and 7 days post-infection, and weekly thereafter. Bioluminescence imaging of nLuc HIV-1 in mice showed an exponential increase in signal between day 3 until week 3-4 post-challenge, including the one mouse with low to undetectable viremia (Figures 3B, 3C). Mouse CR03 did not appear to be productively infected based on plasma viremia, yet nLuc expression was high, suggesting that CD4⁺ cells had been transduced but were not producing virus. However, nLuc expression decreased thereafter in the mice. In vivo fluorescence imaging of iRFP HIV-1 showed a smaller dynamic range compared to nLuc imaging, and iRFP expression peaked at week 3 post-challenge in all of the mice and decreased thereafter to undetectable levels despite having relatively high viremia (Figures 3B, 3C). While in vivo nLuc expression was generally correlated with plasma viremia ($p = 0.025$), in vivo iRFP expression did not correlate with plasma viremia ($p = 0.71$), particularly after week 4 or 5 post-infection (Figure 3D). These data suggest that the reporter viruses replicated in vivo, but reporter gene expression was reduced over time.

Replication and reporter gene expression of the CO reporter viruses were evaluated in humanized mice ($n = 4$ per virus) for up to 15 weeks post-challenge (Figure 2B). In addition, antiretroviral therapy (ART), consisting of daily tenofovir and emtricitabine and weekly long-acting rilpivirine, was administered to the mice between 3-5 weeks post-challenge to suppress virus replication. All animals that were injected with CO-nLuc HIV-1 or CO-iRFP HIV-1 became viremic prior to ART administration (Figure 4A). Plasma viremia was reduced to undetectable or near undetectable levels in all mice during ART. As expected, viremia rebounded in all animals after ART cessation. Viremia rebounded to levels higher than pre-ART, suggesting that reservoirs may not have been completely established at the time of ART administration.

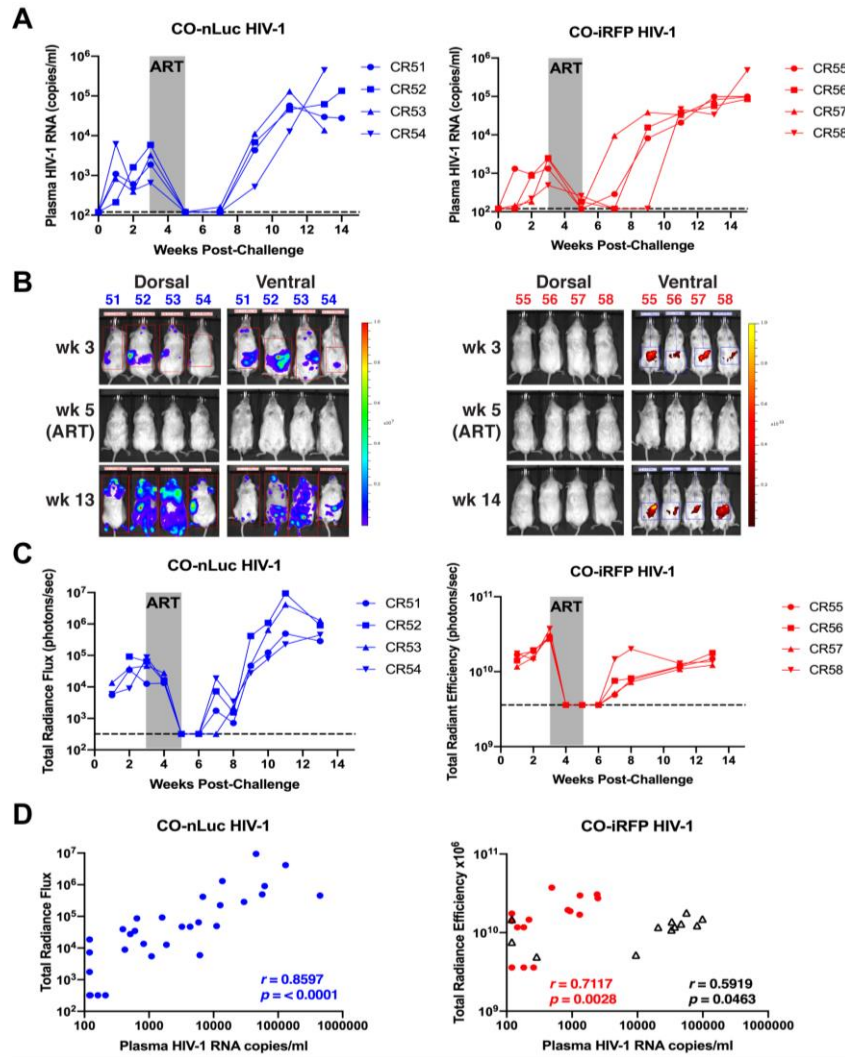


Figure 4. Codon optimization improves in vivo replication of HIV-1 reporter viruses. Humanized mice were challenged with CO-nLuc HIV-1 (n = 4) or CO-iRFP HIV-1 (n = 4). (A) Plasma viremia was measured by qRT-PCR. The limit of detection is denoted by the dashed lines. Grey shading denotes period of ART administration. (B) Images of *in vivo* nLuc or iRFP expression measured by whole body imaging. (C) Expression of *in vivo* nLuc and iRFP expression was quantified at each time point. The limit of detection is denoted by dashed lines. Grey shading denotes period of ART administration. (D) Correlation of reporter gene expression with plasma viremia for all time points are shown. For CO-iRFP HIV-1, data points from weeks 1-5 (red circles) or weeks 7-14 (black triangles) are separated. Spearman's rank correlation coefficient (r) and p values are shown.

In vivo nLuc and iRFP expression was observed in all animals challenged with CO viruses prior to ART and declined to undetectable levels during ART, mimicking the trends seen for plasma viremia (Figures 4B, 4C). Similar to the original iRFP HIV-1 animals, the dynamic range for *in vivo* detection was narrow compared to nLuc. After ART cessation, *in vivo* reporter virus detection increased or remained stable for at least 14 weeks. Reporter expression in animals infected with CO-nLuc HIV-1 correlated more strongly with plasma viremia levels ($p < 0.0001$; Figure 4D) compared to the original reporter virus. Interestingly, the overall correlation between reporter expression and plasma viremia for mice infected with CO-iRFP HIV-1 was not significant ($p = 0.2$). However, if the data points were separated for prior to and during ART (weeks 1-5) or after ART administration (weeks 7-14), the correlation was significant for each data set ($p = 0.0028$ and $p = 0.046$, respectively).

3.3 Removal of CG dinucleotides in reporter genes improved reporter HIV-1 expression in spleen cells of humanized mice

To evaluate expression of the reporters in the original and CO viruses at the cellular level, immunofluorescence was performed on spleens from the animals with productive infection. As animal CR03 did not have appreciable viremia, it was removed from analysis. For animals infected with the nLuc HIV-1 reporter viruses, staining was performed using antibodies against HIV-1 capsid (p24) and nLuc (Figure 5). First, expression intensity of the reporters was assessed and compared to p24 staining intensity. Intensity of spleen p24 staining showed variation between individual cells within a sample and between animals (Figure 6A), but the average mean intensities were nearly identical between the original and CO nLuc HIV-1 groups ($p = 0.97$; Figures 6A, 6B).

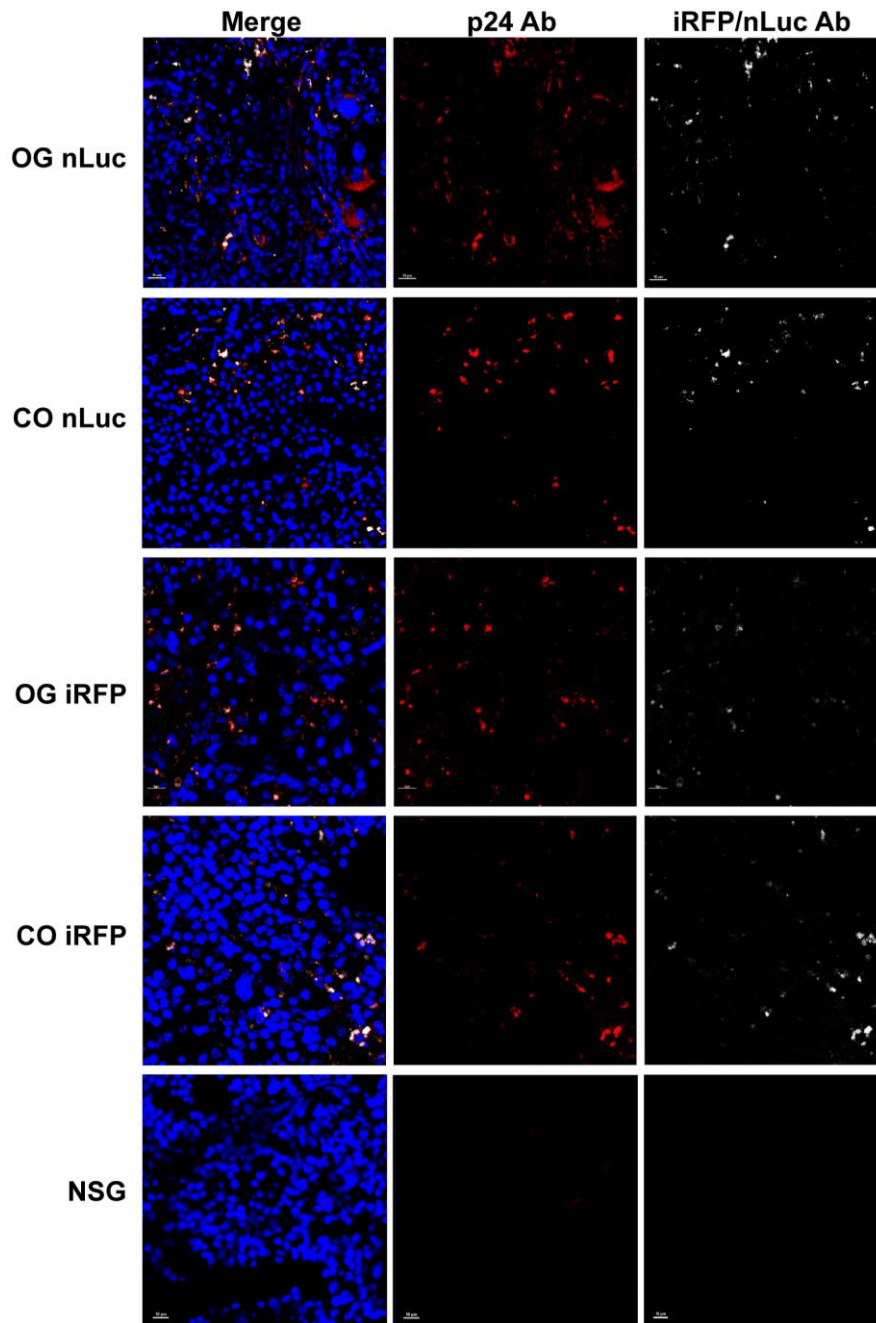


Figure 5. Reporter gene expression can be detected in HIV-1 infected cells in the spleens of humanized mice.

Representative immunofluorescence images of Hoechst (blue), p24 (red), and reporter gene (white) expression in spleen sections of mice infected with original (OG) nLuc HIV-1, CO-nLuc HIV-1, OG iRFP HIV-1, or CO-iRFP HIV-1. A mouse lacking human cells was used as a negative control.

The average intensity of spleen nLuc signal in the animals infected with CO-nLuc HIV-1 was somewhat higher than that in the animals infected with the original reporter virus, but this was

not statistically significant ($p = 0.14$; Figures 6A, 6B). The p24 staining intensity in the spleens of animals infected with the original iRFP HIV-1 was very heterogeneous (Figure 6C) and significantly higher than the animals infected with original nLuc HIV-1 ($p = 0.049$). However, the difference in average mean intensities between animals infected with the original or the CO nLuc HIV-1 was similar ($p = 0.87$; Figures 6C, 6D). In contrast to nLuc expression, iRFP can be visualized without antibodies or substrate (Figure 5). The mean signal intensity was significantly higher in animals infected with CO-iRFP HIV-1 than those infected with the original virus ($p = 0.0081$; Figures 6C, 6D). As immunofluorescence imaging appeared to show some p24+ cells that were not positive for reporter gene expression in animals that were infected with the original reporter viruses, we evaluated the number of p24+ cells that were also positive for reporter expression for all animals. While the frequency of double positive infected cells was on average approximately 50% for animals infected with the original nLuc or iRFP viruses, >90% of p24+ cells also had detectable reporter gene expression in animals infected with the CO reporter viruses (Figure 6E). Overall, the *in vivo* and *ex vivo* data suggest that CG codon optimization of the reporter genes significantly improved their expression.

The intensity of p24 expression was similar in the spleens of mice infected with original or the CO HIV-1 reporter viruses ($p = 0.87$ for iRFP groups; $p = 0.97$ for nLuc groups). This was consistent with plasma viremia levels remaining high for animals infected with either the original or the CO reporter viruses. In contrast, the intensity of iRFP and nLuc expression was greater in the spleens of humanized mice infected with CO HIV-1 reporter virus compared to mice infected with original HIV-1 reporter virus. The difference was greater for iRFP virus ($p = 0.0081$), which originally had 138 CG dinucleotides in the reporter gene, than for nLuc virus ($p = 0.14$), which had 38 CG dinucleotides in the reporter gene.

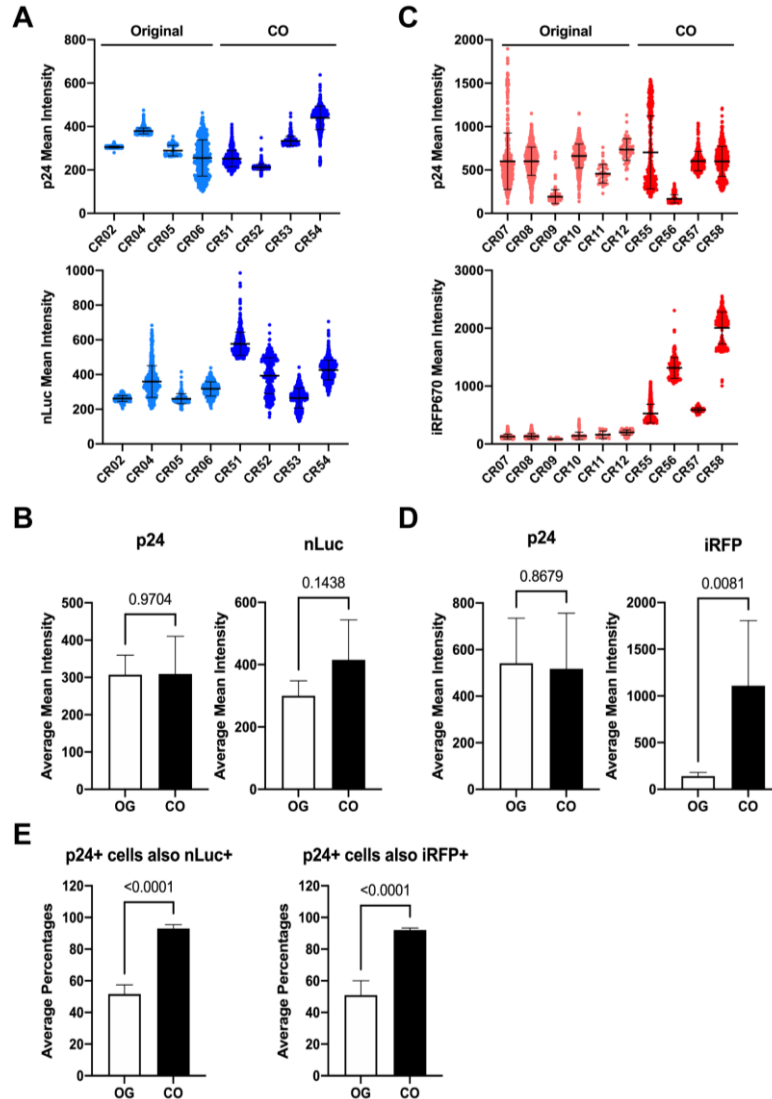


Figure 6. Expression of reporter proteins is improved in spleens of humanized mice infected with codon-optimized HIV-1 reporter viruses. Mean intensities of p24 and reporter gene expression in spleen cells of mice infected with (A) nLuc/CO-nLuc HIV-1 or (C) iRFP/CO-iRFP HIV-1 were measured by immunofluorescence imaging. The average mean intensities of p24 and reporter expression in the (B) nLuc/CO-nLuc HIV-1 or (D) iRFP/CO-iRFP HIV-1 groups are shown. (E) The frequencies of p24+ cells that were also positive for nLuc or iRFP were counted for each animal. The means and standard deviations of each animal or group are shown. The p values from t tests are shown for all bar graphs.

4.0 Discussion

In this study we evaluated HIV-1 infection over time by whole-body imaging in humanized mice using replication-competent molecular clones encoding either a bioluminescent protein (nLuc) or a near-infrared fluorescent protein (iRFP). Both reporter viruses were detectable in humanized mice after infection. Removal of CG dinucleotides increased virus replication levels of both viruses *in vitro*. The iRFP gene is twice the size of the nLuc gene but had more than 3.5-fold the number of CG dinucleotides, which was consistent with greater defects in reporter virus replication and *in vivo* gene expression prior to codon optimization. Removal of CGs significantly improved reporter gene expression *in vivo*. Both the *in vivo* and *ex vivo* expression intensity as well as the correlation of reporter expression in p24+ cells were improved for both reporter viruses after correction of CG dinucleotides.

For the original reporter viruses, *in vivo* nLuc expression was generally correlated with plasma viremia while *in vivo* iRFP expression did not correlate with plasma viremia, showing that the reporter viruses replicated *in vivo* but gene expression was reduced over time. We hypothesized that due to ZAP recognition of CG dinucleotides present in the reporter genes, nLuc and iRFP is removed during replication inside host cells as they are detected as foreign. While plasma viral RNA and intracellular p24 expression were not impaired in the original reporter viruses, reporter expression was significantly decreased, particularly for iRFP HIV-1. As reporter gene expression is derived from the 5' LTR, as are all other viral proteins, it suggests that reporter gene sequences may have been mutated or deleted. This could explain the loss of the reporter signal after 5 weeks despite detectable virus replication. In fact, it has been shown previously that the majority of HIV-

1 proviruses acquire deletions over the course of infection (47, 48). It is possible that the majority of replication-competent viruses in these mice had defective reporter genes.

To overcome this problem, we hypothesized that CG dinucleotides present in the reporter genes led to loss of reporter gene expression. CG codon optimization of HIV-iRFP led to similar intensities of p24 staining and also higher intensities of iRFP expression in the spleens of infected animals compared to the original HIV-iRFP. Codon optimized HIV-nLuc led to similar intensities of p24 staining and nLuc expression in the spleens of infected animals compared to the original HIV-nLuc. Overall, the *in vivo* and *ex vivo* data suggest that CG codon optimization of the reporter genes significantly improved their expression. The fluorescence image analysis methodology successfully quantified the HIV-1 p24 and reporter gene expression in HIV-1 infected mice spleens that can be applicable in other studies. Future *in vivo* imaging studies will be performed using CO reporter viruses.

4.1 Public Health Implications

These results showed that the reporter viruses led to both virus replication and reporter gene expression in cells after infection. By removing CG dinucleotides, HIV-1 infection can be visualized by noninvasive, whole body imaging in mice containing human immune cells over time by reporter expression, which correlates with plasma viremia. The two reporter viruses will provide researchers a tool to develop and study antiretroviral therapy and evaluate HIV-1 persistence and latency. Tracking of both reporter viruses containing different viral sequences may allow investigation of two variants within the same animal, such as wild-type and drug-resistant viruses.

5.0 Bibliography

1. Anonymous. 2016. Global Health Sector Strategy on HIV, 2016-2021 World Health Organization
2. Anonymous. 2021. Epidemiology of HIV National HIV Curriculum
3. Anonymous. 2020. HIV in the United States and Dependent Areas Centers for Disease Control and Prevention
4. Anonymous. 2020. HIV Surveillance Report, 2018 (updated). Centers for Disease and Control
5. Anonymous. 2020. Blacks/African Americans and HIV AETC New England
6. Anuurad E, Semrad A, Berglund L. 2009. Human immunodeficiency virus and highly active antiretroviral therapy-associated metabolic disorders and risk factors for cardiovascular disease. *Metab Syndr Relat Disord* 7:401-10.
7. Goulet JL, Fultz SL, Rimland D, Butt A, Gibert C, Rodriguez-Barradas M, Bryant K, Justice AC. 2007. Aging and infectious diseases: do patterns of comorbidity vary by HIV status, age, and HIV severity? *Clin Infect Dis* 45:1593-601.
8. Cahill S, Valadéz R. 2013. Growing older with HIV/AIDS: new public health challenges. *Am J Public Health* 103:e7-e15.
9. Patel P, Hanson DL, Sullivan PS, Novak RM, Moorman AC, Tong TC, Holmberg SD, Brooks JT. 2008. Incidence of types of cancer among HIV-infected persons compared with the general population in the United States, 1992-2003. *Ann Intern Med* 148:728-36.
10. Anonymous. 2013. HIV Transmission. Centers for Disease Control and Prevention
11. Craigie R, Bushman FD. 2012. HIV DNA integration. *Cold Spring Harb Perspect Med* 2:a006890.
12. Blut A. 2016. Human Immunodeficiency Virus (HIV). *Transfusion Medecine and Hemotherapy* 43:203-222.
13. Anonymous. AIDS and HIV Fact Sheet Maryland Department of Health
14. Ameisen JC. 1994. Programmed cell death (apoptosis) and cell survival regulation: relevance to AIDS and cancer. *Aids* 8:1197-213.
15. Effros RB. 2003. Replicative senescence: the final stage of memory T cell differentiation? *Curr HIV Res* 1:153-65.
16. Roy A, Basak S. 2020. HIV long-term non-progressors share similar features with simian immunodeficiency virus infection of chimpanzees. *J Biomol Struct Dyn* doi:10.1080/07391102.2020.1749129:1-8.
17. Anonymous. Fast Track Commitments to end AIDS by 2030. UNAIDS.
18. Anonymous. 2019. Ending the HIV Epidemic: A plan for America HIV.gov.
19. Grant RM, Lama JR, Anderson PL, McMahan V, Liu AY, Vargas L, Goicochea P, Casapía M, Guanira-Carranza JV, Ramirez-Cardich ME, Montoya-Herrera O, Fernández T, Veloso VG, Buchbinder SP, Chariyalertsak S, Schechter M, Bekker LG, Mayer KH, Kallás EG, Amico KR, Mulligan K, Bushman LR, Hance RJ, Ganoza C, Defechereux P, Postle B, Wang F, McConnell JJ, Zheng JH, Lee J, Rooney JF, Jaffe HS, Martinez AI, Burns DN, Glidden DV. 2010. Preexposure chemoprophylaxis for HIV prevention in men who have sex with men. *N Engl J Med* 363:2587-99.

20. Baeten JM, Donnell D, Ndase P, Mugo NR, Campbell JD, Wangisi J, Tappero JW, Bukusi EA, Cohen CR, Katabira E, Ronald A, Tumwesigye E, Were E, Fife KH, Kiarie J, Farquhar C, John-Stewart G, Kania A, Odoyo J, Mucunguzi A, Nakku-Joloba E, Twesigye R, Ngunjiri K, Apaka C, Tamoo H, Gabona F, Mujugira A, Panteleeff D, Thomas KK, Kidoguchi L, Krows M, Revall J, Morrison S, Haugen H, Emmanuel-Ogier M, Ondrejcek L, Coombs RW, Frenkel L, Hendrix C, Bumpus NN, Bangsberg D, Haberer JE, Stevens WS, Lingappa JR, Celum C. 2012. Antiretroviral prophylaxis for HIV prevention in heterosexual men and women. *N Engl J Med* 367:399-410.
21. Anonymous. 2017. Preeposure Prophylaxis for the prevention of HIV infection in the United States-2017 update Centers for Disease Control and Prevention
22. Anonymous. 2016. Today's HIV?AIDS Epidemic Centers for Disease Control and Prevention
23. Wilson EM, Sereti I. 2013. Immune restoration after antiretroviral therapy: the pitfalls of hasty or incomplete repairs. *Immunol Rev* 254:343-54.
24. Cohen MS, Chen YQ, McCauley M, Gamble T, Hosseinipour MC, Kumarasamy N, Hakim JG, Kumwenda J, Grinsztejn B, Pilotto JH, Godbole SV, Mehendale S, Chariyalertsak S, Santos BR, Mayer KH, Hoffman IF, Eshleman SH, Piwowar-Manning E, Wang L, Makhema J, Mills LA, de Bruyn G, Sanne I, Eron J, Gallant J, Havlir D, Swindells S, Ribaud H, Elharrar V, Burns D, Taha TE, Nielsen-Saines K, Celentano D, Essex M, Fleming TR. 2011. Prevention of HIV-1 infection with early antiretroviral therapy. *N Engl J Med* 365:493-505.
25. Marsden MD, Zack JA. 2010. Establishment and maintenance of HIV latency: model systems and opportunities for intervention. *Future Virol* 5:97-109.
26. Chun TW, Stuyver L, Mizell SB, Ehler LA, Mican JA, Baseler M, Lloyd AL, Nowak MA, Fauci AS. 1997. Presence of an inducible HIV-1 latent reservoir during highly active antiretroviral therapy. *Proc Natl Acad Sci U S A* 94:13193-7.
27. Finzi D, Hermankova M, Pierson T, Carruth LM, Buck C, Chaisson RE, Quinn TC, Chadwick K, Margolick J, Brookmeyer R, Gallant J, Markowitz M, Ho DD, Richman DD, Siliciano RF. 1997. Identification of a reservoir for HIV-1 in patients on highly active antiretroviral therapy. *Science* 278:1295-300.
28. Wong JK, Hezareh M, Gunthard HF, Havlir DV, Ignacio CC, Spina CA, Richman DD. 1997. Recovery of replication-competent HIV despite prolonged suppression of plasma viremia. *Science* 278:1291-5.
29. Marsden MD, Zack JA. 2015. Experimental Approaches for Eliminating Latent HIV. *For Immunopathol Dis Therap* 6:91-99.
30. Ambrose Z. 2012. Use of Animal Models for Anti-HIV Drug Development Intech.
31. Hatzioannou T, Evans DT. 2012. Animal models for HIV/AIDS research. *Nat Rev Microbiol* 10:852-67.
32. Williams KC, Burdo TH. 2009. HIV and SIV infection: the role of cellular restriction and immune responses in viral replication and pathogenesis. *Apmis* 117:400-12.
33. Garcia JV. 2016. Humanized mice for HIV and AIDS research. *Current opinion in virology*, 19:56-64.
34. Mosier DE, Gulizia RJ, Baird SM, Wilson DB. 1988. Transfer of a functional human immune system to mice with severe combined immunodeficiency. *Nature* 335:256-9.
35. Shultz LD, Lyons B. L., Burzenski, L. M., Gott, B., Chen, X., Chaleff, S., Kotb, M., Gillies, S. D., King, M., Mangada, J., Greiner, D. L., & Handgretinger, R. 2005. Human

- lymphoid and myeloid cell development in NOD/LtSz-scid IL2R gamma null mice engrafted with mobilized human hemopoietic stem cells. *Journal of immunology* 170:6477-6489.
36. Watanabe S, Terashima K, Ohta S, Horibata S, Yajima M, Shiozawa Y, Dewan MZ, Yu Z, Ito M, Morio T, Shimizu N, Honda M, Yamamoto N. 2007. Hematopoietic stem cell-engrafted NOD/SCID/IL2Rgamma null mice develop human lymphoid systems and induce long-lasting HIV-1 infection with specific humoral immune responses. *Blood* 109:212-8.
 37. Ventura JD, Beloor J, Allen E, Zhang T, Haugh KA, Uchil PD, Ochsenbauer C, Kieffer C, Kumar P, Hope TJ, Mothes W. 2019. Longitudinal bioluminescent imaging of HIV-1 infection during antiretroviral therapy and treatment interruption in humanized mice. *PLoS Pathog* 15:e1008161.
 38. Stacer AC, Nyati S, Moudgil P, Iyengar R, Luker KE, Rehemtulla A, Luker GD. 2013. NanoLuc reporter for dual luciferase imaging in living animals. *Mol Imaging* 12:1-13.
 39. Isomura M, Yamada K, Noguchi K, Nishizono A. 2017. Near-infrared fluorescent protein iRFP720 is optimal for in vivo fluorescence imaging of rabies virus infection. *J Gen Virol* 98:2689-2698.
 40. Takata MA, Goncalves-Carneiro D, Zang TM, Soll SJ, York A, Blanco-Melo D, Bieniasz PD. 2017. CG dinucleotide suppression enables antiviral defence targeting non-self RNA. *Nature* 550:124-127.
 41. Meagher JL, Takata M, Goncalves-Carneiro D, Keane SC, Rebendenne A, Ong H, Orr VK, MacDonald MR, Stuckey JA, Bieniasz PD, Smith JL. 2019. Structure of the zinc-finger antiviral protein in complex with RNA reveals a mechanism for selective targeting of CG-rich viral sequences. *Proc Natl Acad Sci U S A* 116:24303-24309.
 42. Mariani R, Rasala BA, Rutter G, Wieggers K, Brandt SM, Krausslich HG, Landau NR. 2001. Mouse-human heterokaryons support efficient human immunodeficiency virus type 1 assembly. *J Virol* 75:3141-51.
 43. Alberti MO, Jones JJ, Miglietta R, Ding H, Bakshi RK, Edmonds TG, Kappes JC, Ochsenbauer C. 2015. Optimized Replicating Renilla Luciferase Reporter HIV-1 Utilizing Novel Internal Ribosome Entry Site Elements for Native Nef Expression and Function. *AIDS Res Hum Retroviruses* 31:1278-96.
 44. Cecilia D, KewalRamani VN, O'Leary J, Volsky B, Nyambi P, Burda S, Xu S, Littman DR, Zolla-Pazner S. 1998. Neutralization profiles of primary human immunodeficiency virus type 1 isolates in the context of coreceptor usage. *J Virol* 72:6988-96.
 45. Palmer S, Wiegand AP, Maldarelli F, Bazmi H, Mican JM, Polis M, Dewar RL, Planta A, Liu S, Metcalf JA, Mellors JW, Coffin JM. 2003. New real-time reverse transcriptase-initiated PCR assay with single-copy sensitivity for human immunodeficiency virus type 1 RNA in plasma. *J Clin Microbiol* 41:4531-6.
 46. Melody K, Roy, C. N., Kline, C., Cottrell, M. L., Evans, D., Shutt, K., Pennings, P. S., Keele, B. F., Bility, M., Kashuba, A., & Ambrose, Z. 2020. Long-Acting Rilpivirine (RPV) Preexposure Prophylaxis Does Not Inhibit Vaginal Transmission of RPV-Resistant HIV-1 or Select for High-Frequency Drug Resistance in Humanized Mice. *Journal of Virology* 94.
 47. Ho YC, Shan L, Hosmane NN, Wang J, Laskey SB, Rosenbloom DI, Lai J, Blankson JN, Siliciano JD, Siliciano RF. 2013. Replication-competent noninduced proviruses in the latent reservoir increase barrier to HIV-1 cure. *Cell* 155:540-51.

48. Bruner KM, Murray AJ, Pollack RA, Soliman MG, Laskey SB, Capoferri AA, Lai J, Strain MC, Lada SM, Hoh R, Ho YC, Richman DD, Deeks SG, Siliciano JD, Siliciano RF. 2016. Defective proviruses rapidly accumulate during acute HIV-1 infection. *Nat Med* 22:1043-9.